Unraveling Genomic Complexity at a Quantitative Disease Resistance Locus in Maize

Tiffany M. Jamann,* Jesse A. Poland,†,‡ Judith M. Kolkman,* Laurie G. Smith,§ and Rebecca J. Nelson*,[1]

*School of Integrative Plant Science, Cornell University, Ithaca, New York 14853, †U.S. Department of Agriculture–Agricultural Research Service, Hard Winter Wheat Genetics Research Unit, Manhattan, Kansas 66502, ‡Department of Agronomy, Kansas State University, Manhattan, Kansas 66506, and §Section of Cell and Developmental Biology, Division of Biological Sciences, University of California at San Diego, La Jolla, California 92093

ORCID ID: 0000-0002-9026-7803 (R.J.N.)

ABSTRACT Multiple disease resistance has important implications for plant fitness, given the selection pressure that many pathogens exert directly on natural plant populations and indirectly via crop improvement programs. Evidence of a locus conditioning resistance to multiple pathogens was found in bin 1.06 of the maize genome with the allele from inbred line "Tx303" conditioning quantitative resistance to northern leaf blight (NLB) and qualitative resistance to Stewart's wilt. To dissect the genetic basis of resistance in this region and to refine candidate gene hypotheses, we mapped resistance to the two diseases. Both resistance phenotypes were localized to overlapping regions, with the Stewart's wilt interval refined to a 95.9-kb segment containing three genes and the NLB interval to a 3.60-Mb segment containing 117 genes. Regions of the introgression showed little to no recombination, suggesting structural differences between the inbred lines Tx303 and "B73," the parents of the fine-mapping population. We examined copy number variation across the region using next-generation sequencing data, and found large variation in read depth in Tx303 across the region relative to the reference genome of B73. In the fine-mapping region, association mapping for NLB implicated candidate genes, including a putative zinc finger and *pan1*. We tested mutant alleles and found that *pan1* is a susceptibility gene for NLB and Stewart's wilt. Our data strongly suggest that structural variation plays an important role in resistance conditioned by this region, and *pan1*, a gene conditioning susceptibility for NLB, may underlie the QTL.

THE genes and loci that influence host–pathogen interactions vary in allele effects, specificities, and linkage relationships. While disease resistance can be conditioned by single genes with large effect (Bent 1996; Jones and Dangl 2006), the emerging model of resistance for many plant diseases is complex in nature, with many genes and loci functioning in concert and each contributing a small proportion of the total phenotypic variation (Kump *et al.* 2011; Poland *et al.* 2011; Cook *et al.* 2012b). Each locus has a unique profile, with some loci contributing broad-spectrum protection against diverse pathogen species and strains. Investigating these intricacies offers the opportunity to understand the diverse ways in which plants defend themselves against microbial assault.

Correlated responses to multiple diseases have been observed in various germplasm panels, implying that there are loci and genes that condition broad-spectrum resistance (Rossi *et al.* 2006; Gurung *et al.* 2009; Wisser *et al.* 2011). At the chromosomal segment level, disease and insect resistance loci colocalize in a nonrandom fashion (McMullen and Simcox 1995; Williams 2003; Wisser *et al.* 2005) and loci have been identified that confer resistance to diverse pathogen isolates and taxa (Zwonitzer *et al.* 2010; Chung *et al.* 2011; Belcher *et al.* 2012). There is evidence to suggest that gene clusters can confer resistance to more than one disease. A cluster of germin-like proteins confers resistance to rice blast and sheath blight of rice (Manosalva *et al.* 2009). Similarly, resistance gene homologs, which are known to colocalize with broad-spectrum disease resistance loci, can cluster in the genome and contribute a diversity of specificities (Lopez *et al.* 2003; Ramalingam *et al.* 2003). Pleiotropy remains uncommon in maize, and correlated responses may be due to

doi: 10.1534/genetics.114.167486
Manuscript received April 3, 2014; accepted for publication June 6, 2014; published Early Online July 9, 2014.
Supporting information is available online at http://www.genetics.org/lookup/suppl/doi:10.1534/genetics.114.167486/-/DC1.
[1]Corresponding author: 303G Plant Science Bldg., 236 Tower Rd., Cornell University, Ithaca, NY 14853. E-mail: rjn7@cornell.edu

linkage or population structure (Wallace *et al.* 2014), although in some cases, individual genes have been shown to condition multiple disease resistance (MDR). For example, the putative ABC transporter *Lr34* of wheat provides protection against leaf rust, stripe rust, and powdery mildew (Krattinger *et al.* 2009). Pattern recognition receptors are able to detect molecular patterns from diverse organisms to confer disease resistance (Zipfel and Rathjen 2008).

While in some cases single genes or alleles common across diverse germplasm confer disease resistance, increasingly, the role of structural variation in plants is being explored and its effects on phenotypic variation recognized (Springer *et al.* 2009; Chia *et al.* 2012; McHale *et al.* 2012). As quantitative trait loci (QTL) are subjected to fine mapping, some loci fractionate into many QTL, each conditioned by one or more genes (Steinmetz *et al.* 2002; Studer and Doebley 2011; Johnson *et al.* 2012). In some cases, the allele effect conditioned by each QTL is small enough that the individual locus cannot be identified in isolation (Buckler *et al.* 2009; Poland *et al.* 2011). In other cases, single resistance loci, such as *Rhg1*, are conditioned by multiple genes present in varying copy numbers in different lines (Cook *et al.* 2012a; Maron *et al.* 2013). Whole-genome studies have in fact suggested that structural variation is generally associated with disease resistance: structural variation in plants colocalizes with resistance nucleotide-binding proteins, receptor-like proteins, and disease resistance QTL (Lai *et al.* 2010; McHale *et al.* 2012; Xu *et al.* 2012).

The conventional approach of genetic isolation and transgenic complementation remains the gold standard for demonstrating the function of a gene. This approach, however, is proving inadequate for dealing with the complexity underlying some loci, particularly for structural variation. Strong evidence for the importance of copy number variation in explaining trait variation (Cook *et al.* 2012a; Maron *et al.* 2013) and the emerging model of plant defense with many loci each contributing a small effect combine to challenge this paradigm (Kump *et al.* 2011; Poland *et al.* 2011; Cook *et al.* 2012b). There is a need for a new approach that can take advantage of whole-genome analyses, address presence/absence variation, and examine loci with small effects. This study represents such an approach and provides insights into a genetically complex locus affecting diverse traits.

In maize, chromosomal bin 1.06 has been identified as a key locus for stabilizing yield under adverse conditions, including both biotic and abiotic stress (Landi *et al.* 2002, 2010; Tuberosa *et al.* 2002). In addition to plant architectural traits and yield under abiotic stress, resistance to many diseases has been localized to bin 1.06, including northern leaf blight (NLB), Stewart's wilt, southern leaf blight (SLB), common rust, gray leaf spot (GLS), and ear and stalk rot caused by multiple fungi (Wisser *et al.* 2006; Chung *et al.* 2010b; Zwonitzer *et al.* 2010). In a QTL study of the recombinant inbred line (RIL) population Ki14 × B73 evaluated for three foliar fungal diseases, NLB, GLS, and SLB, a 33-Mb region spanning bins 1.05 and 1.06 was the only locus identified that conferred resistance to all three diseases (Zwonitzer *et al.* 2010). A number of QTL studies for NLB resistance in maize have identified QTL at bin 1.06, ranging in physical size from 3 to 30 Mb (Freymark *et al.* 1993; Welz *et al.* 1999; Wisser *et al.* 2006; Chung *et al.* 2010b, 2011; Van Esbroeck *et al.* 2010; Poland *et al.* 2011). Additionally, bin 1.06 harbors the dominant Stewart's wilt resistance gene *Sw1* (Ming *et al.* 1999).

Both NLB, caused by the fungus *Setosphaeria turcica*, and Stewart's wilt, caused by the bacterium *Pantoea stewartii*, are foliar, hemibiotrophic diseases important to maize production. Both pathogens spread through the vascular tissue, causing wilted lesions by plugging xylem vessels (Jennings and Ullstrup 1957; Roper 2011). The importance of genes localized to maize bin 1.06 in resistance to both NLB and Stewart's wilt has been described in multiple mapping populations. Using a population of Tx303 × B73 introgression lines (Szalma *et al.* 2007), Chung *et al.* (2010b) showed that the NLB resistance QTL at 1.06 protects against fungal penetration.

To explore the genomic complexity of this important region, we constructed high-resolution mapping populations at this locus and evaluated NLB and Stewart's wilt resistance, using a set of Tx303 × B73 near-isogenic lines (NILs) (Szalma *et al.* 2007; Chung *et al.* 2010b). Fine mapping allowed us to dissect the linkage relationship between the major-effect Stewart's wilt QTL and the minor-effect NLB QTL and to identify candidate genes. Using association mapping, we further refined the list of candidate genes for NLB resistance and using mutants confirmed a role for the receptor-like kinase, *pan1*, in plant defense. Furthermore, multiple lines of evidence indicated a lack of genomic stability at the region, including reduced recombination across portions of the fine-mapping region in the NIL population and indicators of copy number variation.

Materials and Methods

Plant materials

The SNP positions used for fine mapping were based on the B73 genome sequence release AGP_V2 (Schnable *et al.*, 2009). NILs used for fine mapping were derived from the **T**x303 × **B**73 **B**ack**c**ross **3** (TBBC3) population, a set of chromosomal segment substitution lines with Tx303 introgressions in a B73 background (Szalma *et al.* 2007; Chung *et al.* 2010b). Chung *et al.* (2010a,b) identified families TBBC3-38 and TBBC3-39, both with introgressions in 1.06, as significantly more resistant than B73. Selected families developed from these lines were chosen for fine mapping: TBBC3-38_19E, TBBC3-38_15G, and TBBC3-38_17A (Chung *et al.* 2010b). The details of population development and evaluation are shown in Supporting Information, Figure S1. Briefly, a population was developed by crossing TBBC3-38_19E to B73. In the F_2 generation, 435 individuals were screened for recombinants with flanking markers snp_01_0042 (180,394,924 bp, AGP_V2) and

snp_01_0005 (195,557,990 bp, AGP_V2). A total of 113 recombinant plants were identified, but seed was available from only 100 plants. Seed from 15 heterozygous F_2 individuals was advanced to the F_3 generation to screen for additional recombinants. A population of 4080 F_3 seeds was planted and 2929 plants were screened with flanking markers snp_01_0042 (180,394,924 bp) and snp_01_0005 (195,557,990 bp). Individual F_3 plants ($n = 874$) were identified as recombinants from the F_3 population. Recombinant plants were self-pollinated and homozygous recombinants identified. Homozygous recombinants were increased and evaluated for disease resistance. Subsequently, a population of 1546 F_3 plants was screened from snp_01_0059 (184,633,349 bp) to snp_01_0083 (189,352,206 bp), yielding an additional 156 recombinants. Homozygous plants were identified, self-pollinated, and screened for NLB and Stewart's wilt (Figure S1).

Disease trials

Northern leaf blight: NLB trials were carried out at the Cornell University Robert Musgrave Research Farm in Aurora, New York. In the fine-mapping populations, 194, 80, and 146 homozygous recombinants were screened for NLB in 2010, 2011, and 2012, respectively. Lines carrying mutations in the genes *pan1* and *pan2* were tested in Aurora, New York in 2011, 2012, and 2013 and in Ithaca, New York in 2011. Plants were inoculated with *S. turcica* isolate StNY001 (race 1), using previously described inoculation procedures (Chung *et al.* 2010a). Briefly, cultures of the fungus were grown on lactose casein agar for 3–4 weeks prior to inoculation or sorghum culturing. A spore suspension was prepared by flooding the cultures with 5 ml sterilized distilled water and conidia were dislodged using a glass rod. The spore suspension was filtered through two layers of cheesecloth and adjusted to a concentration of 4×10^3 spores/ml using a hemocytometer. The spore suspension contained a final concentration of 0.02% Tween 20. Sorghum seed cultures were prepared by soaking 900 ml of sorghum grains in 600 ml distilled water overnight in a 1-gallon clear milk jug and autoclaving twice for 25 min. One milliliter of unfiltered spore suspension was then introduced to each jug, which was then cultured at room temperature for ~3 weeks before field inoculations were conducted. Jugs were shaken daily to prevent caking and provide uniform infestation. For field inoculations, 0.50 ml spore suspension and ~1.25 ml sorghum grains colonized by *S. turcica* were placed into the whorl of each plant at the five- to six-leaf stage.

Diseased leaf area (DLA) was rated on a per row basis three times after flowering at an interval of 7–10 days, using a percentage scale of 0–100 with increments of 1, where 0 indicates a plant with no disease and 100 indicates a completely diseased plant. Area under the disease progress curve (AUDPC) was calculated as described previously (Chung *et al.* 2010a).

Stewart's wilt: Stewart's wilt trials were conducted at the Musgrave Research Farm in Aurora, New York in 2010, 2011, and 2012 for fine mapping and 2012 and 2013 for *pan1* and *pan2* mutants. Results from 2013 were not included in the analysis due to flooding. Plants were inoculated with *P. stewartii* strain PsNY003, originally collected in New York in 1991, at the five- to six-leaf stage, with inoculum prepared and a modified pinprick method used for inoculations as previously described (Chung *et al.* 2010a). DLA was rated on a per row basis at 2–4 weeks after inoculation on a row basis, using a percentage scale of 0–100, with 0 being no disease and 100 being completely diseased.

SNP marker development: The maize diversity project database http://www.panzea.org (Canaran *et al.* 2008) was used to locate polymorphisms between the two inbred lines, using a number of data sets including markers from the nested association mapping (NAM) genetic map (McMullen *et al.* 2009), HapMapV1 (Gore *et al.* 2009), and HapMapV2 (Chia *et al.* 2012). Single-nucleotide polymorphisms (SNPs) polymorphic between B73 and Tx303 were chosen for this study. SNP markers used for the fine-mapping study are shown in Table S1. In addition, an Illumina MaizeSNP50 Beadchip assay was conducted on pooled DNA from families TBBC3-38_05F and TBBC3-38_19E at the David H. Murdock Research Institute (Kannapolis, NC), which included genotypic information for 52,686 SNPs.

DNA extractions: Both Sigma ExNAmp (Sigma-Aldrich) and CTAB DNA extractions were used. ExNAmp DNA extractions were used to identify recombinants and homozygous recombinants. CTAB extractions were used for genotype confirmation and breakpoint analysis. To perform ExNAmp extractions, 1 mm^2 of plant tissue was collected in a 0.2-ml PCR tube and the tubes were placed on ice. Eight microliters of extraction buffer were added to each tube, and tubes were incubated at 95° for 10 min. Following the incubation, 8 μl of dilution buffer was added. The resulting DNA was diluted 1:100 with water for KASPar (LGC Genomics, Hoddesdon, Herfordshire, UK) genotyping. CTAB DNA extractions were performed using ~0.1 mg of fresh tissue as described previously (Doyle and Dickson 1987; Chung *et al.* 2010a).

Allele-specific PCR: When using ExNAmp-extracted DNA, 10 μl of 1:100-diluted DNA was dried down in a 384-well KASPar plate (LGC Genomics) and a 4-μl reaction was performed. For reactions using CTAB-extracted DNA, DNA was quantified and ~5 ng/μl of DNA was used per reaction. Reaction conditions were as follows: 1× KASPar reaction mix (LGC Genomics), 0.4 mM $MgCl_2$, 0.41 mM common reverse primer, and 0.165 μM of each allele-specific primer. Standard oligonucleotides were obtained from IDT (Coralville, IA). PCR thermocycling parameters were as follows: 94° for 15 min; 20 cycles of 94° for 10 sec, 57° for 5 sec, and 72° for 10 sec; followed by 26 cycles of 94° for 10 sec, 57° for 20 sec, and 72° for 40 sec. Results were read using an Applied Biosystems (Foster City, CA) 7900 HT (Life Technologies) and analyzed using SDS v2.1 (Life Technologies).

Experimental design and statistical analysis: A randomized incomplete block design was used for all fine-mapping field experiments, with three replications for NLB trials and two for Stewart's wilt trials. NILs carrying B73 and Tx303 alleles across the region were included in each block as check lines. Two rows were planted around the edge of the experiment to reduce border effects. For the breakpoint analysis, best linear unbiased predictors (BLUPs) were calculated using the "lmer" command in the lme4 package in R version 2.14 (R Development Core Team 2013) where line, year, replication within year, and block nested within replication were fitted as random factors in a mixed-effects model for NLB. Similarly, Stewart's wilt BLUPs were calculated using the lmer command including line and year as random effects. Fine-mapping statistical analyses were completed in R version 2.14 (R Development Core Team 2013), using R/qtl (Broman *et al.* 2003). First, individuals with <11 genotyped markers and markers with <250 individuals genotyped were removed from the analysis. A genetic map was then constructed using the Kosambi mapping function (Kosambi 1943). Single-marker regression was conducted (Paterson *et al.* 1990; Kump *et al.* 2010), using the "scanone" function in R/qtl. Confidence intervals were calculated on the basis of a 95% Bayes credible interval, using the function "bayesint" in R/qtl (Broman *et al.* 2003). Genotypes and phenotypes can be found in File S1.

Recombination rate diversity: Recombination rates were calculated using genotyping-by-sequencing SNPs on the NAM subpopulations, using phased and fully imputed at 1-cM resolution genotypes (AllZea_GBSv2.3) (http://panzea.org/lit/data_sets.html). Genetic maps were constructed using R/qtl with the "est.map" function in R (Broman *et al.* 2003; R Development Core Team 2013).

Read depth variation: Illumina single- and paired-end sequencing reads averaging $\sim 4\times$ coverage of the genome, generated as part of the HapMapV1 and V2 projects (NCBI accession SRA051245), were used for the read depth variation analysis (Chia *et al.* 2012). Aligned sequencing reads for B73 and Tx303 (Chia *et al.* 2012) were downloaded from iPlant (Goff *et al.* 2011). SAMtools was used to count the number of reads at each nucleotide location (Li *et al.* 2009). A Perl script was written to divide the interval into 11 bins of equal size (327,181 bp) and to compile the number of reads per bin.

Candidate gene identification: All B73 RefGenV2 (AGP_V2) filtered genes between the two flanking markers snp_01_0047 at 185,737,089 bp (AGP_V2) and snp_01_0082 at 189,336,643 bp (AGP_V2) of the narrowed NLB fine-mapping interval were considered as candidate genes. SNPs from genome-wide nested association mapping with a bootstrap posterior probability (BPP) > 0.01 that fell within the narrowed fine-mapping interval were considered further as candidates (Poland *et al.* 2011; Chia *et al.* 2012).

Association analysis of the 282-line maize diversity panel: Association mapping was conducted for the NLB fine-mapping interval. BLUPs that included design factors, flowering time, and population structure were used for association analysis (Wisser *et al.* 2011). A mixed linear model (MLM) was implemented using TASSEL v4 (Bradbury *et al.* 2007). The markers assayed included 47,445 Illumina MaizeSNP50 SNPs (Cook *et al.* 2012b) and 425,035 genotyping-by-sequencing SNPs (Romay *et al.* 2013), filtered to remove sites with $>20\%$ missing data (Olukolu *et al.* 2013). The kinship (K) matrix was constructed in TASSEL, using a 5000-SNP subset of the Illumina MaizeSNP50 data set that had no missing data (Olukolu *et al.* 2013). Q-values were calculated using the qvalue package (Storey 2002). Associations with a false discovery rate (FDR) < 0.15 were noted.

Mutant analysis: Mutants in the *pan1* and *pan2* genes were evaluated for NLB and Stewart's wilt reaction. Two mutant alleles of *pan1* were evaluated in a B73 background: one mutant generated by ethyl methanesulfonate mutagenesis (*pan1-EMS*) and one line with a *Mutator1* (*Mu1*) transposon in *pan1* (Gallagher and Smith 2000; Cartwright *et al.* 2009). Two ethyl methanesulfonate alleles of *pan2* were evaluated in a B73 background: *pan2-O* and *pan2-3* (Cartwright *et al.* 2009). All *pan1* and *pan2* mutant alleles except *pan2-O* can be considered null alleles based on the nature of the mutations and analysis of PAN protein accumulation in mutants, whereas *pan2-O* is a missense allele that may encode a partially functional protein (Cartwright *et al.* 2009). *pan1* mutant lines were backcrossed to B73 three to five times and *pan2* mutants were backcrossed to B73 three to seven times. For mutant analysis a complete block design was used, with five replications per location for *pan1* and *pan2* mutants. NLB results were analyzed with a mixed linear model in JMP 9.0 (SAS, Cary, NC), with genotype as a fixed effect and replication nested within environment and environment as random effects. Stewart's wilt results were analyzed with genotype as a fixed effect and replication as a random effect.

RT-PCR analysis: Tissue for RNA extraction was collected from mature leaf tissue of $(BC_4F_3)BC_1F_5$ plants carrying either the B73 ($qNLB1.06_{B73}$) or the Tx303 allele ($qNLB1.06_{Tx303}$) at the *qNLB1.06* locus during the summers of 2011 and 2012. RNA was extracted using an RNeasy kit (QIAGEN, Valencia, CA) and first cDNA was prepared from this RNA, using a RETROscript First-Strand cDNA Synthesis kit (Life Technologies). PCR was carried out using primers for amplification of *pan1* (5′-TCGGGATGGAGCTGGAGGAG-3′ and 5′-TGGACAGACGCACGGACCAC-3′) and actin as a control (5′-TCAGCAGGTCTTCTCTTTCTT-3′ and 5′-TCCTTCA TATTTCCTTCGTTC-3′) with Q5 Hot Start Taq Polymerase (New England Biolabs, Beverly, MA). *pan1* and actin PCR products were quantified from gel images, using NIH ImageJ v. 1.47g.

Results

Identification of MDR in bin 1.06

A number of QTL studies have localized resistance to NLB to maize bin 1.06, with varying resolution (Table S2). These studies have consistently implicated the region spanning from 180 to 205 Mb. Lines carrying a Tx303 introgression at this interval were found to be associated with resistance to NLB and Stewart's wilt (families TBBC3-38 and TBBC-39 of the TBBC3 population) (Chung *et al.* 2010b). Based on genetic background and seed availability, TBBC3-38_19E, TBBC3-38_15A, and TBBC3-38_17G were selected for fine mapping. The Tx303 introgression in TBBC3-38 spans from ss196428597 (172,877,033 bp) to ss196518155 (196,244,799 bp) (Figure 1). An interval of 15.16 Mb spanning from snp_01_0042 (180,394,890 bp, AGP_V2) to snp_01_0005 (195,557,990 bp, AGP_V2) was targeted for fine mapping, based on NIL introgression locations and previous QTL mapping studies (Table S2 and Figure 1).

Fine mapping of MDR at 1.06

Two markers flanking the *qNLB1.06* region, snp_01_0042 and snp_01_0005, were used to screen 435 F_2 and 4475 F_3 plants. We identified a total of 1130 recombinants spanning the 15-Mb interval of interest. Plants were self-pollinated and progeny were assayed for homozygous (fixed) recombinants. Recombinant plants were selected for phenotypic evaluation based on breakpoint analysis and seed availability. Fixed recombinants were screened for disease phenotype in a randomized incomplete block design with two control NILs, one carrying the B73 allele and one carrying the Tx303 allele in the region of interest. Fixed recombinants were screened for NLB (n = 194, 80, and 146 in 2010, 2011, and 2012, respectively) and Stewart's wilt (n = 60, 78, and 140 in 2010, 2011 and 2012, respectively) (Figure 1). An additional 17 SNP markers were assayed on the population to determine the physical position of breakpoints (Table S1). Five were removed from the breakpoint analysis because of missing genotypes or a lack of recombination with neighboring markers. The order of the physical map matched the order of the genetic map. Based on these data, *qNLB1.06* was narrowed to a 3.60-Mb region flanked by snp_01_0047 (185,737,089 bp) and snp_01_0082 (189,336,643 bp) (Figure 1). *qSw1.06* was narrowed to a 95.9-kb interval flanked by snp_01_0137 (187,245,104 bp) and snp_01_0139 (187,341,010 bp) (Figure 1). While confidence intervals differed for the diseases, breakpoint analyses for both showed similar profiles.

Genomic integrity

We observed a low frequency of recombination across part of the fine-mapping region. To determine whether this was an anomaly found only in the NIL fine-mapping population, we examined the recombination rates across the RIL populations that compose the NAM population by examining genetic distances in NAM subpopulations, as shown in Figure 2. We found a depressed recombination rate across portions of the target interval in the Tx303 × B73 RIL population, confirming a low rate of recombination found in the current study between B73 and Tx303 in this region. Furthermore, most NAM founder lines showed low recombination rates across parts of the region. Hp301, however, showed slightly higher levels of recombination, suggesting structural similarity between B73 and Hp301. Other lines, such as Ms71 and M37W, showed repressed recombination in other regions of the interval.

Because low recombination rates are hypothesized to be due to structural variation such as inversions, indels, transposable elements, or presence/absence variation (McMullen *et al.* 2009), we examined Illumina reads from the HapMapV2 project (Chia *et al.* 2012) to assess read depth variation as a proxy for structural variation. We found variation in the number of Tx303 reads that mapped to the B73 reference sequence, while little variation was observed in the number of B73 reads that mapped to the reference sequence (Figure 3). The region with little to no recombination in the NAM subpopulations showed a reduced number of reads in Tx303. Conversely, the region with significant copy number variation (CNV) in the NAM genome-wide association study (GWAS) associations at (187 Mb) had an elevated number of reads that mapped to the reference genome in this location, suggesting possible duplications and genome expansion.

Candidate genes underlying $qSw1.06_{Tx303}$

The Stewart's wilt fine-mapping region was narrowed to a 95.9-kb interval that contains three genes in the B73 reference: a putative zinc finger (GRMZM2G445684) and two uncharacterized genes (GRMZM2G445676, and AC213857.4_FG001). The two uncharacterized genes have no known homologs and no annotated domains. Resistance at this locus is conferred by Tx303, and it is therefore plausible that the resistance gene is absent from the B73 reference.

Candidate genes underlying $qNLB1.06_{Tx303}$

The fine-mapping region falling within the Bayes 95% confidence interval for NLB resistance, 185.7–189.3 Mb of maize chromosome 1, comprises 117 annotated coding genes, 30 pseudogenes, and 39 transposable elements in the B73 genome sequence (Table S3). A number of genes within the narrowed fine-mapping interval are credible candidates based on the involvement of those gene classes in plant defense as documented in the scientific literature. These include three putative leucine-rich repeat-encoding genes, three putative protein kinases, two putative wall-associated receptor kinases, and one putative lipoxygenase sharing homology with *Arabidopsis thaliana LOX2*. Furthermore, genome-wide nested association mapping conducted by Chia *et al.* (2012) identified three significant associations clustered within the 40-kb region spanning 187.23–187.27 Mb AGP_V1. The most significant hit was an intergenic 10-kb read depth variation with a BPP of 44, which was

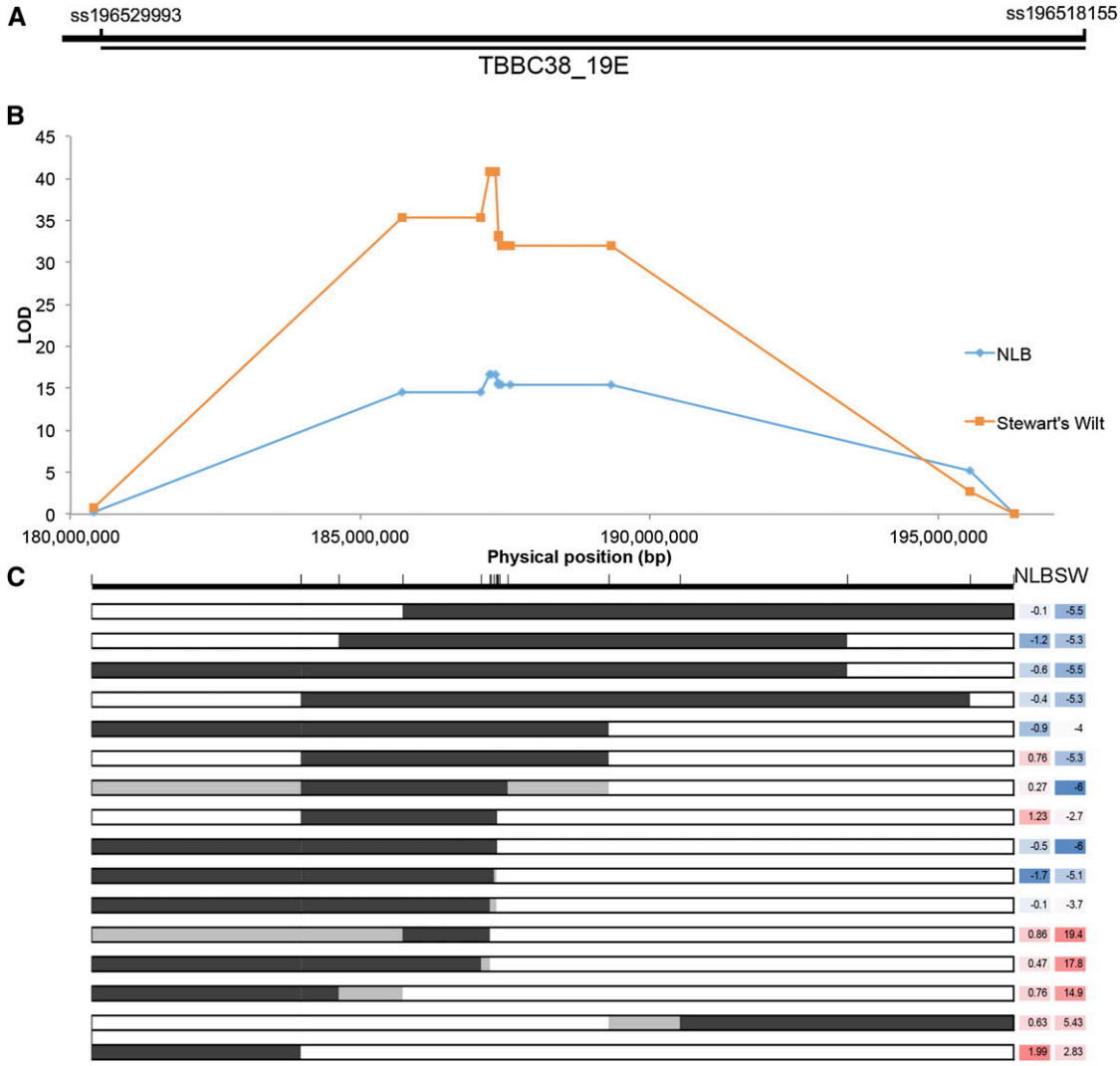

Figure 1 Mapping of *qNLB1.06* and breakpoint analyses for *qNLB1.06*. (A) Location of introgression TBBC3_19E is shown with marker names. (B) Breakpoint analysis for NLB and Stewart's wilt. (C) Selected representative recombinants and their associated phenotypes. For genotypes, dark shading indicates the Tx303 allele, while white indicates the B73 allele. Light gray shading indicates the region of a recombination event. For phenotypes, blue shading indicates a more resistant line, while red indicates a more susceptible line.

30 kb upstream of a putative serine–threonine protein kinase and 129 kb downstream of a putative zinc-finger encoding gene (GRMZM2G441903). Two additional polymorphisms, one intronic SNP (BPP = 3) and one intergenic copy number variation (BPP = 1), were within 40 kb of the significant association with BPP = 44.

Association mapping

Association analysis of this region using the 282-line Goodman diversity panel (Flint-Garcia *et al.* 2005) evaluated for NLB (Wisser *et al.* 2011) identified an association between 185.7 Mb and 189.3 Mb (Figure 4). For significant intergenic associations, adjacent genes were considered as well as genes implicated by long-distance linkage disequilibrium. The SNP implicated by association analysis was located at 188,018,070 bp (AGP_V2) (P-value = 1.72×10^{-4}, q-value = 0.136), 260 bp downstream of a SpoU methylase (GRMZM5G854901) and 13.54 kb upstream of an uncharacterized gene with a helix-loop-helix DNA-binding domain (GRMZM5G879527). The receptor-like kinase *pan1* (GRMZM5G836190) is located 37.555 kb from the significant diversity panel association, a distance close enough to link the SNP to *pan1* by long-range linkage disequilibrium (Chia *et al.* 2012), or the SNP could implicate a downstream element regulating the expression of *pan1*.

pan1 is a susceptibility gene for NLB

pan1 (GRMZM5G836190 at position 187,978,007–187,980,232 on chromosome 1) was initially a candidate gene for disease resistance at 1.06 based on its location inside the fine-mapping interval, its proximity to an NLB association from the diversity panel analysis, and its identity as a receptor-like kinase (Cartwright *et al.* 2009) [this class of proteins is known to detect microbe-associated molecular patterns

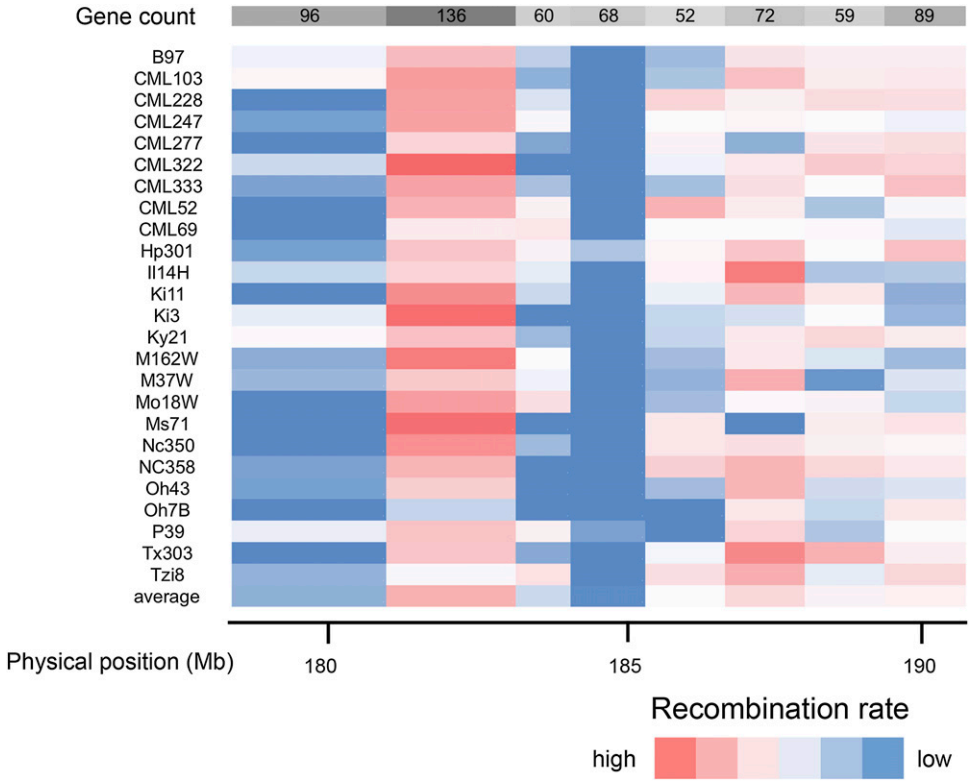

Figure 2 Recombination rates across the fine-mapping interval. Recombination rates were calculated between nine markers for the NAM subpopulations. NAM founders are shown on the left and the gene counts for the eight subintervals are across the top. Red indicates regions of high recombination and blue indicates regions of low recombination.

(Zipfel 2008)]. Phenotypically similar, but unlinked, *pan2* mutants (Zhang *et al.* 2012) were also assessed to test the hypothesis that the *pan* genes influence the disease response through their known effect on stomatal morphology or related pathways. We tested *pan1* and *pan2* mutants for NLB and Stewart's wilt in replicated, multiyear trials and found a significant genotype effect (*P*-value <0.0001) for both diseases. Both mutants with null alleles of *pan1* were found to be significantly more resistant to both diseases than B73, indicating *pan1* is a susceptibility gene for NLB and Stewart's wilt, while *pan2* mutants showed no significant difference from B73 (Figure 5). For NLB, *pan1-Mu* had a 41% decrease in AUDPC, compared with B73, and was generally more resistant than *pan1-ems*, which had a 27% decrease in AUDPC, compared with B73. For Stewart's wilt, *pan1* mutants were nearly immune.

These results suggest that partial or complete loss of *pan1* may contribute to the increased resistance to NLB seen for $qNLB1.06_{Tx303}$ compared to $qNLB1.06_{B73}$. We examined the gene action of the QTL and in two different environments found that the QTL acted in a dominant fashion, where the heterozygote NIL fell into the same phenotypic class as the resistant NIL carrying two copies of the Tx303 allele. Preliminary data from one environment showed that the *pan1-ems* mutation was also dominant for resistance. Further data are needed to confirm this observation. To further test whether *pan1* underlies *qNLB1.06*, we compared *pan1* gene expression levels in mature leaves of these two lines via RT-PCR. Consistent with reduced *pan1* function in $qNLB1.06_{Tx303}$, we found *pan1* to control actin signal ratios were decreased from 0.915 ± 0.168 in $qNLB1.06_{B73}$ to 0.553 ± 0.035 in $qNLB1.06_{Tx303}$ ($\pm$ standard errors, $P < 0.05$ using Student's *t*-test). However, further work will be needed to determine whether the reduction in *pan1* expression level in $qNLB1.06_{Tx303}$ is causally related to the increase in NLB resistance seen in this line.

Discussion

Loci that underlie a number of traits present an opportunity to investigate the complex relationship between variation for traits, genome structure, recombination, and causative genes. Maize bin 1.06 is one such locus that is associated with effects on diverse traits. This chromosomal region of interest has been described as a yield-stabilizing locus associated with effects on resistance to several diseases, root architecture, plant height, flowering time, and yield across different soil moisture levels and genetic backgrounds (Landi *et al.* 2002, 2010; Tuberosa *et al.* 2002; Wisser *et al.* 2006). This locus is a relatively QTL-dense segment of the maize genome, with more than double the average number of QTL (35 QTL *vs.* an average of 15 QTL per bin), but of average genetic size based on the NAM genetic map and based on physical size (McMullen *et al.* 2009; Andorf *et al.* 2010). The elevated number of QTL in this bin, coupled with an average gene content and genetic size, indicates that this bin is important for maize breeding across a broad set of traits. Hence, it is of interest not only to identify the genes underlying those traits, including MDR, but also to investigate the genome dynamics shaping the region.

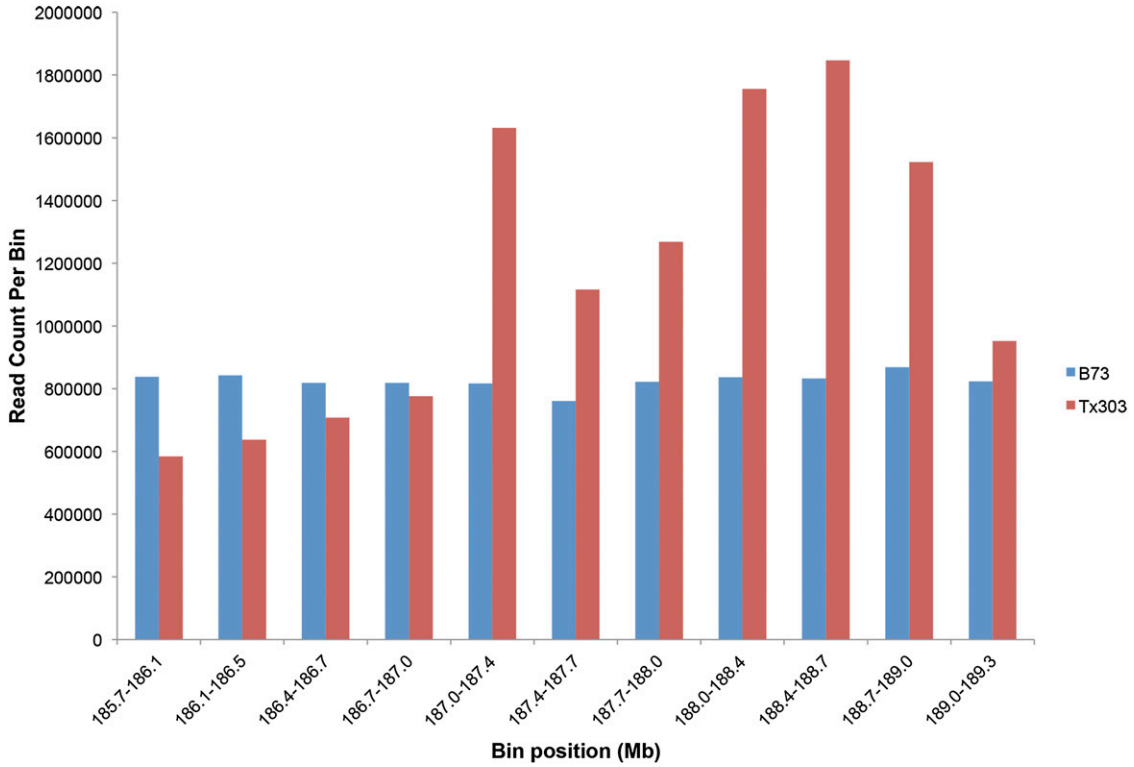

Figure 3 Read depth variation across the *qNLB1.06* fine-mapping region. Blue bars indicate the number of B73 Illumina reads that align to the given bin, while red bars indicate the number of Tx303 Illumina reads that align to the given bin. Bins are 327 kb and the start position of the bin in noted on the *x*-axis.

Consistent with the observation of high QTL density, variations in the targeted interval were shown to be under selection during domestication and subsequent varietal improvement. Candidate genes for domestication syndrome in this region, identified as genes lying in extended regions with allele frequency differentiation between landraces and *Zea mays* ssp. *parviglumis*, include genes such as a putative lipoxygenase, putative frataxin, and a putative zinc finger among others, while "improvement candidates" (those that contrast for improved lines *vs.* landraces) include putative protein kinases, putative EF-hand proteins, a putative alcohol dehydrogenase, and a putative antifreeze protein, among others (Hufford *et al.* 2012). The observed patterns of selection may be related to disease resistance, as the transcriptional rewiring of the maize transcriptome during domestication suggests that genes related to biotic stress are overrepresented among the group of genes upregulated during domestication (Swanson-Wagner *et al.* 2012). Indeed, some of these candidate genes, such as lipoxygenase, serine/threonine protein kinase, and the antifreeze protein, could be involved in one of the many disease resistances conditioned by this locus.

This region harboring numerous QTL for diverse traits shows signs of high genome complexity and plasticity. A low recombination rate in the fine-mapping interval was observed in the NILs, with a limited number of recombinants identified between 184.6 Mb and 187.6 Mb, but an average gene density compared to the maize genome as a whole (Schnable *et al.* 2009). The fine-mapping interval, including the region of low recombination, colocalizes with the yield-stabilizing QTL reported by Landi *et al.* (2010). A reduced recombination rate in this interval was observed in many of the NAM subpopulations, providing support for the hypothesis that B73 has a lack of synteny with other maize lines at this region, with the exception of Hp301, which recombines with B73 in this region. The low recombination could be due to small inversions, indels, transposon insertion, or prescence/absence variation (McMullen *et al.* 2009). Such differences that suppress recombination may be selected upon to conserve the yield-stabilizing haplotype located at this region.

Increasingly, CNV has been found to underlie trait variation, including biotic and abiotic stress tolerance (Cook *et al.* 2012a; Maron *et al.* 2013). A CNV polymorphism was significantly associated with NLB in the 1.06 interval based on the NAM GWAS. Together with the lack of recombination in part of the fine-mapping population, this suggests that genome content variation across diverse maize germplasm may underlie the differences in disease response. To test this hypothesis, structural differences were explored by examining read depth variation across the region. Pronounced variation in the number of Tx303 reads that mapped to the reference was found, which can be interpreted as evidence for duplications or genome expansion at this region in Tx303. This is not uncommon, as the maize genome is

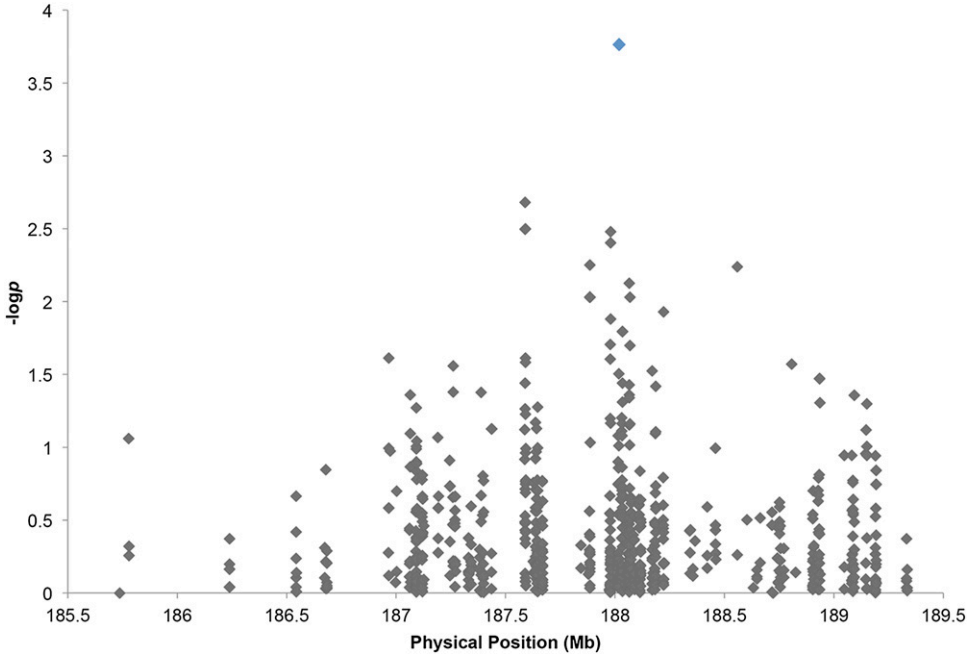

Figure 4 Diversity panel association. Shown is association analysis for NLB in the fine-mapping region using the Goodman diversity panel (Flint-Garcia *et al.* 2005; Wisser *et al.* 2011). The significant SNP at 188,018,070 bp (*P*-value = 1.72×10^{-4}, *q*-value = 0.136) is highlighted in blue.

highly plastic, with read depth variation in 90% of the genome (Chia *et al.* 2012) and presence/absence variation thought to be a major driver of phenotypic variation in maize (Wallace *et al.* 2014).

Given the complex genetic basis of quantitative traits and this region, a fine-mapping approach was taken to refine the genomic region associated with resistance to NLB and Stewart's wilt, complemented by association mapping to identify candidate genes. The fine-mapping approach allowed for the dissection of the multitrait nature of this QTL. Resistance to Stewart's wilt was localized to a 95.9-kb region within the larger 3.60-Mb NLB fine-mapping interval. While the majority of major QTL have been shown not to be pleiotropic in nature (Wallace *et al.* 2014), a pleiotropic basis of disease resistance cannot be excluded at this locus. The breakpoint analysis for both diseases was similar, although the confidence interval of NLB was calculated to be larger than that for Stewart's wilt.

The candidate region for Stewart's wilt contains three genes in the B73 genome sequence: a gene with a putative zinc finger and two uncharacterized genes. Both uncharacterized genes lack homologs and one lacks expression evidence (Dong *et al.* 2004; Sen *et al.* 2010). However, the genic content of the region may differ in Tx303. A physical map assembly for Tx303 across the fine-mapping region would clarify this. A number of mapping studies have implicated the region on chromosome 1 between 180 and 190 Mb across diverse populations for resistance to NLB. The *qNLB1.06*$_{Tx303}$ region has been successfully narrowed to 3.6 Mb. While 117 candidate genes from the B73 genome sequence were implicated through fine mapping, it is again likely that Tx303 differs in the genic content of this region. A subset of the NLB candidate genes was particularly credible based on previous knowledge of plant defense, including four putative leucine-rich repeat protein kinases. Other candidates include a putative frataxin, a putative ABC transporter, and a putative lipoxygenase.

Association mapping provides a complementary approach for identifying candidate genes. Significant associations within the *qNLB1.06*$_{Tx303}$ fine-mapping interval were detected using both the NAM and Goodman diversity panels (Flint-Garcia *et al.* 2005; Poland *et al.* 2011; Wisser *et al.* 2011; Chia *et al.* 2012). The most significant association within this region in the NAM was an intergenic copy number variation, which had a BPP value of 44 (*P*-value = 0.0000737), one of the most highly significant associations from the analysis (Poland *et al.* 2011; Chia *et al.* 2012). Among the genes implicated by NAM, the putative A20/AN1 zinc finger was the strongest candidate, a gene domain that is associated with stress tolerance in plants and the immune system in animals (Vij and Tyagi 2008). This polymorphism is close to the Stewart's wilt fine-mapping interval, lending support to the hypothesis that a region present in Tx303 but not B73 may contain gene(s) for resistance to both diseases. Association analysis using the Goodman diversity panel revealed a significant intergenic SNP within the fine-mapping interval, ~800 kb from the NAM CNV (Flint-Garcia *et al.* 2005; Wisser *et al.* 2011). The NLB-associated CNV and SNP polymorphisms may be in linkage disequilibrium with one or more genes in the vicinity. Candidate genes from association mapping can be further investigated through expression analyses, resequencing, and testing across different germplasm sets.

Within the fine-mapping interval shown in Figure 1, the significant Goodman panel SNP was 38 kb from *pan1*. We tested the *pan* mutants for both NLB and Stewart's wilt because the mapping results for the two diseases were similar (Figure 1). The smaller confidence interval for Stewart's wilt may

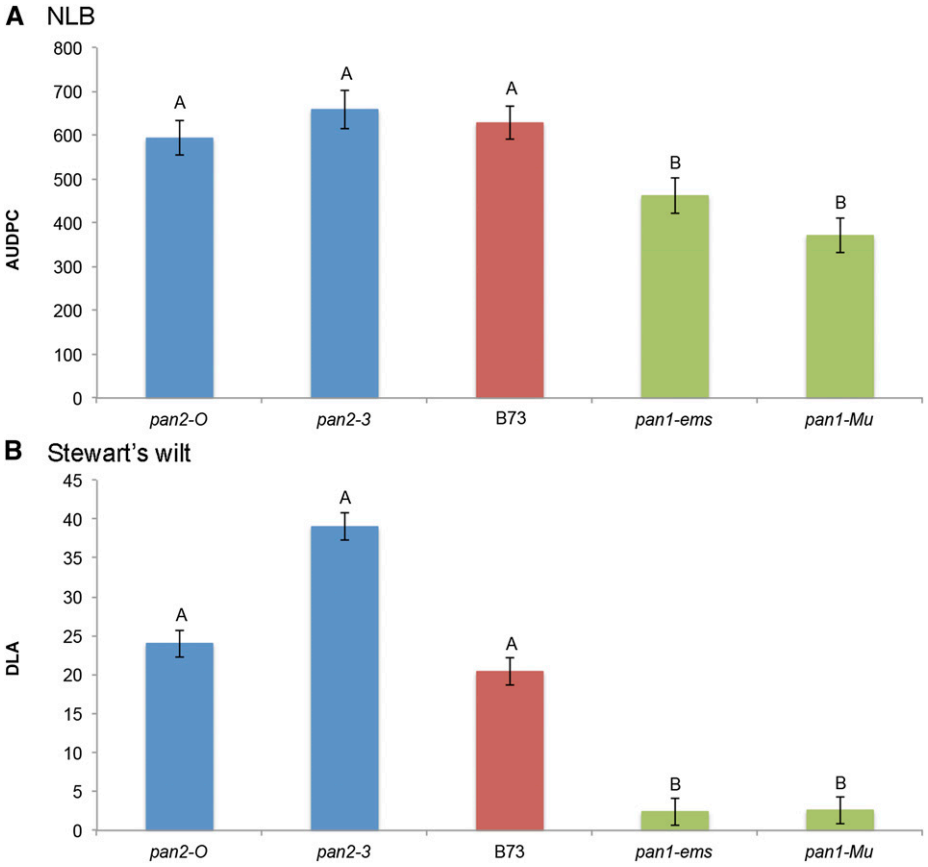

Figure 5 (A) NLB disease response of mutants. (B) Stewart's wilt response of mutants. In both A and B plants homozygous for both *pan*1-ems and *pan*1-Mu alleles are significantly different from B73, the background for the mutants, while pan2 mutants are not. Letters denote significance with Student's *t*-test (*P*-value, 0.0001). *pan*2 mutants are shown in blue, while *pan*1 mutants are shown in green. B73 is shown in red.

reflect the stronger phenotype, while the similar profile indicates that there may be multiple genes underlying the QTL for both diseases. Two independent null mutant alleles of this gene conferred resistance phenotypes for NLB and Stewart's wilt (Figure 5), demonstrating that mutations in *pan1* itself (not a linked gene present in one or the other mutant background) increase resistance for the two diseases. This finding suggests that a loss-of-function allele of *pan1* derived from Tx303 may contribute to the disease resistance phenotype(s) conferred by $qNLB1.06_{Tx303}$ and $qSW1.06_{Tx303}$. Preliminary data showed that the QTL and *pan1* mutants showed similar inheritance patterns with dominant resistance in both cases. This is unexpected for a loss-of-function mutation. Further work is needed to confirm the gene action of the *pan1* mutants and to dissect the relationship between the MDR QTL and *pan1*.

PAN1 has been shown to play a role in promoting features of actin organization that support asymmetric cell division (Cartwright *et al.* 2009). Interestingly, lines carrying mutations for *pan2*, which also show asymmetric cell division, were not significantly different from B73 for NLB, indicating aberrant stomata found in both mutant lines are not the underlying mechanism of resistance in the *pan1* mutants. Susceptibility conditioned by wild-type *pan1* could be due to a passive mechanism, such as altered anatomical structures, or an active process, such as actin reorganization during pathogen attack.

We have successfully refined $q1.06_{Tx303}$, identified candidate genes, and demonstrated a role for *pan1* in multiple disease resistance. NLB and Stewart's wilt resistance regions have been narrowed sufficiently that the markers within the NLB and Stewart's wilt intervals can be used for marker-assisted selection. These data strongly suggest that structural variation underlies this locus and *pan1*, a gene in which lowered expression is correlated with higher resistance levels, may underlie the NLB and Stewart's wilt QTL. Loss of susceptible *pan1* alleles could be used to decrease maize susceptibility to diverse pathogens. Through fine mapping, examining recombination rates and resequencing data, and evaluating mutant lines, we were able to dissect a complex locus and identified a role for *pan1* in plant defense. This approach has shed light on a locus known for its complexity and quantitative effect.

Acknowledgments

We acknowledge Santiago Mideros for bioinformatics support and Randall Wisser, Bode Olukolu, and Chia-Lin Chung for helpful discussions and technical assistance. We acknowledge Laura Morales, Alyssa Cowles, William Miller, Chris Mancuso, Katharine Constas, Ariel Fialko, and Xingyu Luo for their assistance with fieldwork and Yeri Park for help with the *pan1* RT-PCR experiments. This work was funded by National Science Foundation award 1127076, the McKnight Foundation, the Cornell University Agricultural Experiment Station federal

formula funds, Project No. NYC-153418 received from the National Institute of Food and Agriculture (NIFA), United States Department of Agriculture, and Cornell University. Any opinions, findings, conclusions, or recommendations expressed in the publication are those of the author(s) and do not necessarily reflect the view of the National Institute of Food and Agriculture (NIFA), of the United States Department of Agriculture (USDA), or of the other funders.

Literature Cited

Andorf, C. M., C. J. Lawrence, L. C. Harper, M. L. Schaeffer, D. A. Campbell *et al.*, 2010 The locus lookup tool at MaizeGDB: identification of genomic regions in maize by integrating sequence information with physical and genetic maps. Bioinformatics 26: 434–436.

Belcher, A. R., J. C. Zwonitzer, J. Santa Cruz, M. D. Krakowsky, C. L. Chung *et al.*, 2012 Analysis of quantitative disease resistance to southern leaf blight and of multiple disease resistance in maize, using near-isogenic lines. Theor. Appl. Genet. 124: 433–445.

Bent, A. F., 1996 Plant disease resistance genes: function meets structure. Plant Cell 8: 1757–1771.

Bradbury, P. J., Z. Zhang, D. E. Kroon, T. M. Casstevens, Y. Ramdoss *et al.*, 2007 TASSEL: software for association mapping of complex traits in diverse samples. Bioinformatics 23: 2633–2635.

Broman, K. W., H. Wu, S. Sen, and G. A. Churchill, 2003 R/qtl: QTL mapping in experimental crosses. Bioinformatics 19: 889–890.

Buckler, E. S., J. B. Holland, P. J. Bradbury, C. B. Acharya, P. J. Brown *et al.*, 2009 The genetic architecture of maize flowering time. Science 325: 714–718.

Canaran, P., E. S. Buckler, J. C. Glaubitz, L. Stein, Q. Sun *et al.*, 2008 Panzea: an update on new content and features. Nucleic Acids Res. 36: D1041–D1043.

Cartwright, H. N., J. A. Humphries, and L. G. Smith, 2009 PAN1: a receptor-like protein that promotes polarization of an asymmetric cell division in maize. Science 323: 649–651.

Chia, J. M., C. Song, P. J. Bradbury, D. Costich, N. de Leon *et al.*, 2012 Maize HapMap2 identifies extant variation from a genome in flux. Nat. Genet. 44: 803–807.

Chung, C. L., T. Jamann, J. Longfellow, and R. Nelson, 2010a Characterization and fine-mapping of a resistance locus for northern leaf blight in maize bin 8.06. Theor. Appl. Genet. 121: 205–227.

Chung, C. L., J. M. Longfellow, E. K. Walsh, Z. Kerdieh, G. Van Esbroeck *et al.*, 2010b Resistance loci affecting distinct stages of fungal pathogenesis: use of introgression lines for QTL mapping and characterization in the maize-*Setosphaeria turcica* pathosystem. BMC Plant Biol. 10: 103.

Chung, C. L., J. Poland, K. Kump, J. Benson, J. Longfellow *et al.*, 2011 Targeted discovery of quantitative trait loci for resistance to northern leaf blight and other diseases of maize. Theor. Appl. Genet. 123: 307–326.

Cook, D. E., T. G. Lee, X. Guo, S. Melito, K. Wang *et al.*, 2012a Copy number variation of multiple genes at *Rhg1* mediates nematode resistance in soybean. Science 338: 1206–1209.

Cook, J. P., M. D. McMullen, J. B. Holland, F. Tian, P. Bradbury *et al.*, 2012b Genetic architecture of maize kernel composition in the nested association mapping and inbred association panels. Plant Physiol. 158: 824–834.

Dong, Q., S. D. Schlueter, and V. Brendel, 2004 PlantGDB, plant genome database and analysis tools. Nucleic Acids Res. 32: D354–D359.

Doyle, J. J., and E. E. Dickson, 1987 Preservation of plant samples for DNA restriction endonuclease analysis. Taxon 36: 715–722.

Flint-Garcia, S. A., A. C. Thuillet, J. Yu, G. Pressoir, S. M. Romero *et al.*, 2005 Maize association population: a high-resolution platform for quantitative trait locus dissection. Plant J. 44: 1054–1064.

Freymark, P. J., M. Lee, W. L. Woodman, and C. A. Martinson, 1993 Quantitative and qualitative trait loci affecting host-plant response to *Exserohilum turcicum* in maize (*Zea mays L.*). Theor. Appl. Genet. 87: 537–544.

Gallagher, K., and L. G. Smith, 2000 Roles for polarity and nuclear determinants in specifying daughter cell fates after an asymmetric cell division in the maize leaf. Curr. Biol. 10: 1229–1232.

Goff, S. A., M. Vaughn, S. McKay, E. Lyons, A. E. Stapleton *et al.*, 2011 The iPlant Collaborative: cyberinfrastructure for plant biology. Front. Plant Sci. 2: 34.

Gore, M. A., J. M. Chia, R. J. Elshire, Q. Sun, E. S. Ersoz *et al.*, 2009 A first-generation haplotype map of maize. Science 326: 1115–1117.

Gurung, S., J. M. Bonman, S. Ali, J. Patel, M. Myrfield *et al.*, 2009 New and diverse sources of multiple disease resistance in wheat. Crop Sci. 49: 1655–1666.

Hufford, M. B., X. Xu, J. van Heerwaarden, T. Pyhajarvi, J. M. Chia *et al.*, 2012 Comparative population genomics of maize domestication and improvement. Nat. Genet. 44: 808–811.

Jennings, P., and A. Ullstrup, 1957 A histological study of three Helminthosporium leaf blights of corn. Phytopathology 47: 707–714.

Johnson, E. B., J. E. Haggard, and D. A. St Clair, 2012 Fractionation, stability, and isolate-specificity of QTL for resistance to *Phytophthora infestans* in cultivated tomato (*Solanum lycopersicum*). G3 2: 1145–1159.

Jones, J. D., and J. L. Dangl, 2006 The plant immune system. Nature 444: 323–329.

Kosambi, D. D., 1943 The estimation of map distances from recombination values. Ann. Eugen. 12: 172–175.

Krattinger, S. G., E. S. Lagudah, W. Spielmeyer, R. P. Singh, J. Huerta-Espino *et al.*, 2009 A putative ABC transporter confers durable resistance to multiple fungal pathogens in wheat. Science 323: 1360–1363.

Kump, K. L., P. J. Bradbury, R. J. Wisser, E. S. Buckler, A. R. Belcher *et al.*, 2011 Genome-wide association study of quantitative resistance to southern leaf blight in the maize nested association mapping population. Nat. Genet. 43: 163–168.

Kump, K., J. Holland, M. Jung, P. Wolters, and P. Balint-Kurti, 2010 Joint analysis of near-isogenic and recombinant inbred line populations yields precise positional estimates for quantitative trait loci. Plant Genome 3: 142–153.

Lai, J., R. Li, X. Xu, W. Jin, M. Xu *et al.*, 2010 Genome-wide patterns of genetic variation among elite maize inbred lines. Nat. Genet. 42: 1027–1030.

Landi, P., M. Sanguineti, L. Darrah, M. Giuhani, S. Salvi *et al.*, 2002 Detection of QTLs for vertical root pulling resistance in maize and overlap with QTLs for root traits in hydroponics and for grain yield under different water regimes. Maydica 47: 233–243.

Landi, P., S. Giuliani, S. Salvi, M. Ferri, R. Tuberosa *et al.*, 2010 Characterization of *root-yield-1.06*, a major constitutive QTL for root and agronomic traits in maize across water regimes. J. Exp. Bot. 61: 3553–3562.

Li, H., B. Handsaker, A. Wysoker, T. Fennell, J. Ruan *et al.*, 2009 The Sequence Alignment/Map format and SAMtools. Bioinformatics 25: 2078–2079.

Lopez, C. E., I. F. Acosta, C. Jara, F. Pedraza, E. Gaitan-Solis *et al.*, 2003 Identifying resistance gene analogs associated with resistances to different pathogens in common bean. Phytopathology 93: 88–95.

Manosalva, P. M., R. M. Davidson, B. Liu, X. Zhu, S. H. Hulbert *et al.*, 2009 A germin-like protein gene family functions as a complex quantitative trait locus conferring broad-spectrum disease resistance in rice. Plant Physiol. 149: 286–296.

Maron, L. G., C. T. Guimaraes, M. Kirst, P. S. Albert, J. A. Birchler *et al.*, 2013 Aluminum tolerance in maize is associated with higher *MATE1* gene copy number. Proc. Natl. Acad. Sci. USA 110: 5241–5246.

McHale, L. K., W. J. Haun, W. W. Xu, P. B. Bhaskar, J. E. Anderson *et al.*, 2012 Structural variants in the soybean genome localize to clusters of biotic stress-response genes. Plant Physiol. 159: 1295–1308.

McMullen, M. D., and K. D. Simcox, 1995 Genomic organization of disease and insect resistance genes in maize. Mol. Plant Microbe Interact. 8: 811–815.

McMullen, M. D., S. Kresovich, H. S. Villeda, P. Bradbury, H. Li *et al.*, 2009 Genetic properties of the maize nested association mapping population. Science 325: 737–740.

Ming, R., J. Brewbaker, H. Moon, T. Musket, R. Holley *et al.*, 1999 Identification of RFLP markers linked to a major gene, *sw1*, conferring resistance to Stewart's wilt in maize. Maydica 44: 319–323.

Olukolu, B. A., A. Negeri, R. Dhawan, B. P. Venkata, P. Sharma *et al.*, 2013 A connected set of genes associated with programmed cell death implicated in controlling the hypersensitive response in maize. Genetics 193: 609–620.

Paterson, A., J. DeVerna, B. Lanini, and S. Tanksley, 1990 Fine mapping of quantitative trait loci using selected overlapping recombinant chromosomes, in an interspecies cross of tomato. Genetics 124: 735–742.

Poland, J. A., P. J. Bradbury, E. S. Buckler, and R. J. Nelson, 2011 Genome-wide nested association mapping of quantitative resistance to northern leaf blight in maize. Proc. Natl. Acad. Sci. USA 108: 6893–6898.

R Development Core Team, 2013 *R: A Language and Environment for Statistical Computing*. R Foundation for Statistical Computing, Vienna.

Ramalingam, J., C. M. Vera Cruz, K. Kukreja, J. M. Chittoor, J. L. Wu *et al.*, 2003 Candidate defense genes from rice, barley, and maize and their association with qualitative and quantitative resistance in rice. Mol. Plant Microbe Interact. 16: 14–24.

Romay, M. C., M. J. Millard, J. C. Glaubitz, J. A. Peiffer, K. L. Swarts *et al.*, 2013 Comprehensive genotyping of the USA national maize inbred seed bank. Genome Biol. 14: R55.

Roper, M. C., 2011 *Pantoea stewartii* subsp. *stewartii*: lessons learned from a xylem-dwelling pathogen of sweet corn. Mol. Plant Pathol. 12: 628–637.

Rossi, C., A. Cuesta-Marcos, I. Vales, L. Gomez-Pando, G. Orjeda *et al.*, 2006 Mapping multiple disease resistance genes using a barley mapping population evaluated in Peru, Mexico, and the USA. Mol. Breed. 18: 355–366.

Schnable, P. S., D. Ware, R. S. Fulton, J. C. Stein, F. Wei *et al.*, 2009 The B73 maize genome: complexity, diversity, and dynamics. Science 326: 1112–1115.

Sen, T. Z., L. C. Harper, M. L. Schaeffer, C. M. Andorf, T. E. Seigfried *et al.*, 2010 Choosing a genome browser for a Model Organism Database: surveying the maize community. Database 2010: baq007.

Springer, N. M., K. Ying, Y. Fu, T. Ji, C. T. Yeh *et al.*, 2009 Maize inbreds exhibit high levels of copy number variation (CNV) and presence/absence variation (PAV) in genome content. PLoS Genet. 5: e1000734.

Steinmetz, L. M., H. Sinha, D. R. Richards, J. I. Spiegelman, P. J. Oefner *et al.*, 2002 Dissecting the architecture of a quantitative trait locus in yeast. Nature 416: 326–330.

Storey, J. D., 2002 A direct approach to false discovery rates. J. R. Stat. Soc. Ser. B Stat. Methodol. 64: 479–498.

Studer, A. J., and J. F. Doebley, 2011 Do large effect QTL fractionate? A case study at the maize domestication QTL *teosinte branched1*. Genetics 188: 673–681.

Swanson-Wagner, R., R. Briskine, R. Schaefer, M. B. Hufford, J. Ross-Ibarra *et al.*, 2012 Reshaping of the maize transcriptome by domestication. Proc. Natl. Acad. Sci. USA 109: 11878–11883.

Szalma, S. J., B. M. Hostert, J. R. Ledeaux, C. W. Stuber, and J. B. Holland, 2007 QTL mapping with near-isogenic lines in maize. Theor. Appl. Genet. 114: 1211–1228.

Tuberosa, R., M. C. Sanguineti, P. Landi, M. Michela Giuliani, S. Salvi *et al.*, 2002 Identification of QTLs for root characteristics in maize grown in hydroponics and analysis of their overlap with QTLs for grain yield in the field at two water regimes. Plant Mol. Biol. 48: 697–712.

Van Esbroeck, G., M. E. Smith, P. J. Balint-Kurti, J. Jung, and J. Yang, 2010 Use of a maize advanced intercross line for mapping of QTL for northern leaf blight resistance and multiple disease resistance. Crop Sci. 50: 458–466.

Vij, S., and A. K. Tyagi, 2008 A20/AN1 zinc-finger domain-containing proteins in plants and animals represent common elements in stress response. Funct. Integr. Genomics 8: 301–307.

Wallace, J. G., S. J. Larsson, and E. S. Buckler, 2014 Entering the second century of maize quantitative genetics. Heredity 112: 30–38.

Welz, H. G., X. C. Xia, P. Bassetti, A. E. Melchinger, and T. Lubberstedt, 1999 QTLs for resistance to *Setosphaeria turcica* in an early maturing Dent x Flint maize population. Theor. Appl. Genet. 99: 649–655.

Williams, K. J., 2003 The molecular genetics of disease resistance in barley. Aust. J. Agric. Res. 54: 1065.

Wisser, R. J., Q. Sun, S. H. Hulbert, S. Kresovich, and R. J. Nelson, 2005 Identification and characterization of regions of the rice genome associated with broad-spectrum, quantitative disease resistance. Genetics 169: 2277–2293.

Wisser, R. J., P. J. Balint-Kurti, and R. J. Nelson, 2006 The genetic architecture of disease resistance in maize: a synthesis of published studies. Phytopathology 96: 120–129.

Wisser, R. J., J. M. Kolkman, M. E. Patzoldt, J. B. Holland, J. Yu *et al.*, 2011 Multivariate analysis of maize disease resistances suggests a pleiotropic genetic basis and implicates a GST gene. Proc. Natl. Acad. Sci. USA 108: 7339–7344.

Xu, X., X. Liu, S. Ge, J. D. Jensen, F. Hu *et al.*, 2012 Resequencing 50 accessions of cultivated and wild rice yields markers for identifying agronomically important genes. Nat. Biotechnol. 30: 105–111.

Zhang, X., M. Facette, J. A. Humphries, Z. Shen, Y. Park *et al.*, 2012 Identification of PAN2 by quantitative proteomics as a leucine-rich repeat-receptor-like kinase acting upstream of PAN1 to polarize cell division in maize. Plant Cell 24: 4577–4589.

Zipfel, C., 2008 Pattern-recognition receptors in plant innate immunity. Curr. Opin. Immunol. 20: 10–16.

Zipfel, C., and J. P. Rathjen, 2008 Plant immunity: *AvrPto* targets the frontline. Curr. Biol. 18: R218–R220.

Zwonitzer, J. C., N. D. Coles, M. D. Krakowsky, C. Arellano, J. B. Holland *et al.*, 2010 Mapping resistance quantitative trait loci for three foliar diseases in a maize recombinant inbred line population-evidence for multiple disease resistance? Phytopathology 100: 72–79.

Communicating editor: D. Zamir

GENETICS

Supporting Information
http://www.genetics.org/lookup/suppl/doi:10.1534/genetics.114.167486/-/DC1

Unraveling Genomic Complexity at a Quantitative Disease Resistance Locus in Maize

Tiffany M. Jamann, Jesse A. Poland, Judith M. Kolkman, Laurie G. Smith, and Rebecca J. Nelson

DOI: 10.1534/genetics.114.167486

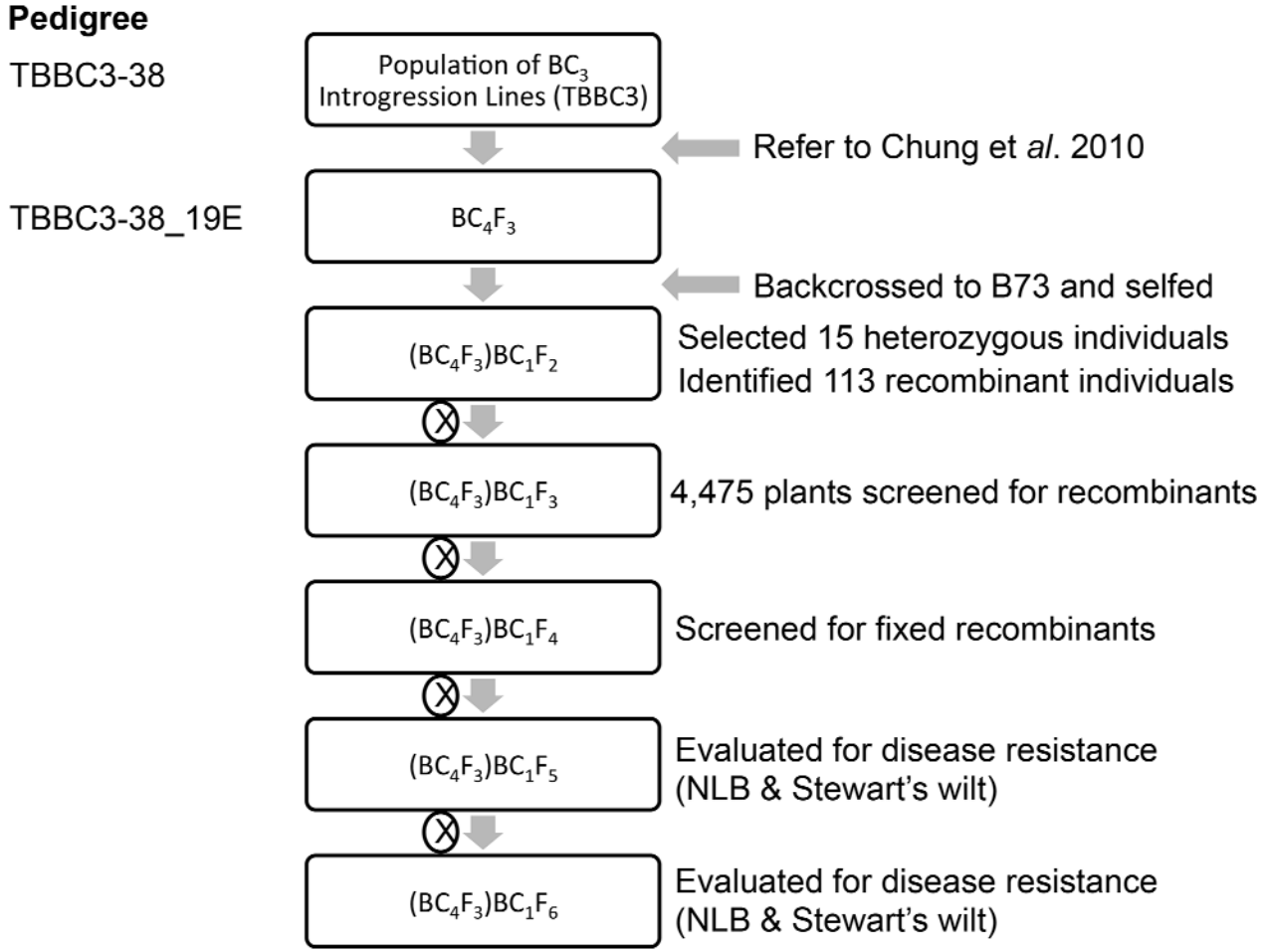

Figure S1 Near-isogenic line development. Near-isogenic line development is shown beginning with population development by Szalma et *al*. (2007) and Chung et *al*. (2010), through homozygous recombinant screening.

File S1

Genotypic and phenotypic data for fine-mapping study

Available for download as an Excel file at http://www.genetics.org/lookup/suppl/doi:10.1534/genetics.114.167486/-/DC1

Table S1 Markers

Marker ID	Locus name	Physical position*	Forward primer 1	Forward primer 2	Common reverse primer
snp_01_0042	ch1_AC202158_78820	180,394,890	GAAGGTGACCAAGTTCATGC TGCCGATACCAATCACTGACA	GAAGGTCGGAGTCAACGGATTCTGC CGATACCAATCACTGACG	GCCCCGGTCGGTACACAGTTA
snp_01_0057	chr1|183107525|C/T	184,016,638	GAAGGTGACCAAGTTCATGC TCCCTCACCAGCGACCACC	GAAGGTCGGAGTCAACGGATTCTTC CCTCACCAGCGACCACT	GGCAGGCAAGGTCACAGAGGAA
snp_01_0015	PZA00068.1	183,986,082	GAAGGTGACCAAGTTCATGC TGACAGGGAACCGGATTCTA TAG	GAAGGTCGGAGTCAACGGATTGTG ACAGGGAACCGGATTCTATAA	GTTAATCTTCACCTGGTGCATCGTG TA
snp_01_0059	chr1|184516928|G/A	184,633,349	GAAGGTGACCAAGTTCATGC TCCAGGGCCTGCTAACGCTGT T	GAAGGTCGGAGTCAACGGATTCAG GGCCTGCTAACGCTGTC	CGTACATGTGCCGCGCGTTTATATA
snp_01_0047	chr1|185582569|A/C	185,737,089	GAAGGTGACCAAGTTCATGC TGAATTGCTATTATTATATAA CTCAACCCGT	GAAGGTCGGAGTCAACGGATTAATT GCTATTATTATATAACTCAACCCGG	TCGGCCATCTCGGCAACCTCAA
snp_01_0136	ss229502009	187,090,230	GAAGGTGACCAAGTTCATGC TGCAATAACCATTGAACCAAC GAC	GAAGGTCGGAGTCAACGGATTCTGC AATAACCATTGAACCAACGAG	GTCCAGCTATAGGATAGGAAGAGC AT
snp_01_0137	ss229502244	187,245,104	GAAGGTGACCAAGTTCATGC TGCGTCATTTTCTCGTCAGGG C	GAAGGTCGGAGTCAACGGATTCTGC GTCATTTTCTCGTCAGGGA	ACTCCATTATTCATGCTTGATGGAC CTA
snp_01_0138	ss229502327	187,272,680	GAAGGTGACCAAGTTCATGC TACTGCTAGCAGCTACTGCAG G	GAAGGTCGGAGTCAACGGATTCTAC TGCTAGCAGCTACTGCAGA	CCAACCTTTACCTAAACATGTTTGC TGTT
snp_01_0139	ss229502401	187,341,010	GAAGGTGACCAAGTTCATGC TGCGCCTCTCCTCCACGGC	GAAGGTCGGAGTCAACGGATTGCG CCTCTCCTCCACGGT	ACGGTGCCCGGCGCGTGAA
snp_01_0115	ss229502466	187,399,046	GAAGGTGACCAAGTTCATGC TCGTAACGGCAAGCTTCTCTG TGT	GAAGGTCGGAGTCAACGGATTGTA ACGGCAAGCTTCTCTGTGC	TCTCTGGCGTAGGGTCCTCTCT

snp_01_0116	ss229502486	187,400,044	GAAGGTGACCAAGTTCATGC TTCCGCTGCCGCTGCGGA	GAAGGTCGGAGTCAACGGATTCCGC TGCCGCTGCGGG	GCAGTCGTGGCGGTCCGAGTA
snp_01_0117	ss229502506	187,401,161	GAAGGTGACCAAGTTCATGC TGGACAGCGAACCCGGGGA	GAAGGTCGGAGTCAACGGATTGGA CAGCGAACCCGGGGG	CCTTGGTCGCGTCTGGCTGCT
snp_01_0118	ss229502527	187,436,581	GAAGGTGACCAAGTTCATGC TTTGTTAAGCAAGCACACAGA AGCG	GAAGGTCGGAGTCAACGGATTTGTT AAGCAAGCACACAGAAGCA	CAGCTGCTCGTCGTCTGTTGTTAAT
snp_01_0079	ss196501884	187,588,467	GAAGGTGACCAAGTTCATGC TACCGGAACATCGTCAAGAT GGAA	GAAGGTCGGAGTCAACGGATTCCG GAACATCGTCAAGATGGAG	CGGAGAGGATCACGCCGAAGTT
snp_01_0082	ss229504554	189,336,643	GAAGGTGACCAAGTTCATGC TCCTTGCGCTCTCAGGTTTTT GCA	GAAGGTCGGAGTCAACGGATTCTTG CGCTCTCAGGTTTTTGCG	TCATTCAGGTGGGCCCAGGCT
snp_01_0083	ss196429231	189,352,206	GAAGGTGACCAAGTTCATGC TCAGCCCCCTCTGTCCGTT	GAAGGTCGGAGTCAACGGATTCAG CCCCCTCTGTCCGTC	CCTTCAAGCTCGAGCTGGGACT
snp_01_0085	ss196516288	190,594,339	GAAGGTGACCAAGTTCATGC TGTTTAAGAATTGGATATCAT TGATCGAC	GAAGGTCGGAGTCAACGGATTCTGT TTAAGAATTGGATATCATTGATCGA T	GGCGTTGCTGATATCGCGTTCAATT
snp_01_0061	chr1|193313487|C/T	193,478,836	GAAGGTGACCAAGTTCATGC TGGTTCGTCCATTGCCGGAAT C	GAAGGTCGGAGTCAACGGATTCGG TTCGTCCATTGCCGGAATT	CGAACTCAACAGAGGAATTCTTAC CTT
snp_01_0005	PZA00619.3	195,557,990	GAAGGTGACCAAGTTCATGC TGAAGCACTCAACGCCGCCA GA	GAAGGTCGGAGTCAACGGATTAGC ACTCAACGCCGCCAGG	GMCATGCATATATATATGGCTGCC TCAT
snp_01_0088	ss229511302	196,306,976	GAAGGTGACCAAGTTCATGC TGATGTCCATGAATTTTCCAG TTCCAA	GAAGGTCGGAGTCAACGGATTGAT GTCCATGAATTTTCCAGTTCCAT	AGCTCAGTACACTAGTAAAAATTA GGGTAA

*Physical positions are AGP_V2.

Table S2 NLB QTL mapping studies.

Reference	Parents	Resistance source	Population	QTL mapping	Trait	Flanking markers		Lower CI*	Upper CI*
Balint-Kurti *et al.* 2010	B73 x Mo17	B73	RIL	Composite interval mapping	AUDPC (AU06WMD)	bnlg1598	umc1396	187.8	191.1
Freymark *et al.* 1993	B52 x Mo17	B52	$F_{2:3}$	Interval mapping	Average Number of lesions/leaf	umc157	umc67	12.2	175.6
					Average percentage leaf tissue diseased	umc157	umc67	12.2	175.6
Welz *et al.* 1999	D32 x D145	D32	F_3	Composite interval mapping	% diseased leaf area	csu61b	dup12 (dupssr12)	181.0	239.6
Wisser *et al.* 2008	-	-	Recurrent selection	Selection mapping	-	bnlg615		201.0	
Chung *et al.* 2010	B73 x Tx303	Tx303	NILs	-	IP, AUDPC	umc1754	umc2234	180.0	187.4
Chung *et al*. 2011	B73 x CML52	CML52	HIFs	-	IP, lesion number, diseased leaf area, AUDPC			182.6	189.8
	B73 x CML52	CML52	RIL	ICIM	3 diseased leaf area ratings			200.4	205.8
Zwonitzer *et al.* 2010	Ki14 × B73	Ki14	RIL	Multiple interval mapping	sAUDPC	PZA01041.2	bnlg1057	157.1	190.0
Poland *et al.* 2011	NAM	B97 CML103 CML247 CML52 CML69	NAM	Joint linkage mapping	AUDPC	PZA02191.1	PZA00619.3	182.5	195.6

Ki11	
Ki3	
M37W	
Mo17	
Mo18W	
NC358	
Tzi8	

Previous QTL studies that identified QTL for NLB resistance at maize bin 1.06 are listed. Confidence interval (CI) locations are based on AGP_V2.

Table S3 Candidate genes

Gene ID	Start (AGP_V2)	Stop (AGP_V2)	Interpro Description
GRMZM2G119511	185735951	185738575	Pyridoxal phosphate-dependent transferase
GRMZM2G419430	185737836	185738414	Calcium-binding EF-hand
GRMZM2G419431	185739064	185740761	
GRMZM2G419436	185739619	185740699	Serine/threonine-protein kinase, active site
GRMZM2G119547	185741603	185742128	Actin cross-linking
GRMZM2G124428	185777384	185779013	Wall-associated receptor kinase galacturonan-binding domain
AC190935.2_FG001	186007538	186008047	
GRMZM2G116254	186214773	186215342	Calcium-binding EF-hand
GRMZM2G552586	186230672	186232165	Aldehyde/histidinol dehydrogenase
GRMZM2G116236	186236715	186237201	
GRMZM2G417360	186237596	186238072	HAT dimerisation
AC186416.3_FG001	186340690	186342603	
GRMZM2G037493	186468876	186472999	SANT/Myb domain
GRMZM2G037581	186533673	186537407	WD40 repeat
GRMZM2G502940	186538248	186538450	
AC215187.3_FG003	186593280	186593915	
AC205695.3_FG008	186615110	186616941	
GRMZM2G362303	186633675	186639255	Protein kinase, catalytic domain
GRMZM2G308597	186640159	186640742	Calcium-binding EF-hand
GRMZM2G449226	186652945	186655618	
GRMZM2G391281	186674312	186675233	
GRMZM2G391288	186675613	186678029	S-receptor-like serine/threonine-protein kinase
GRMZM5G811972	186678239	186678787	
AC208564.3_FG004	186736360	186737646	Transcription factor, K-box
GRMZM2G061739	186964841	186965674	
AC211887.3_FG001	186964865	186965437	
GRMZM5G832154	186972934	186973635	
GRMZM5G800323	186973040	186973858	
GRMZM2G061791	186995763	186999056	
GRMZM2G359559	187002125	187004115	Aminotransferase, class V/Cysteine desulfurase
AC211887.3_FG004	187003702	187004115	Calcium-binding EF-hand
GRMZM2G059012	187055101	187062082	Wall-associated receptor kinase galacturonan-binding domain
AC211887.3_FG006	187063931	187064597	

GRMZM2G359434	187065602	187069942	Pentatricopeptide repeat
AC211887.3_FG007	187065698	187066120	Calcium-binding EF-hand
GRMZM2G059129	187091607	187095345	Glycerophosphoryl diester phosphodiesterase
GRMZM2G085210	187118709	187121135	Proton-dependent oligopeptide transporter family
GRMZM2G119381	187179081	187180794	
GRMZM2G419267	187190806	187194254	Glycosyltransferase AER61, uncharacterised
GRMZM2G445684	187269130	187271929	Zinc finger, C2H2
GRMZM2G445676	187271948	187272122	
AC213857.4_FG001	187338417	187341110	
GRMZM2G083755	187341766	187344871	Frataxin/CyaY
GRMZM2G083803	187344872	187345544	
AC213857.4_FG003	187344907	187345239	EF-Hand 1, calcium-binding site
GRMZM2G552850	187353437	187354156	
AC212463.3_FG001	187368059	187379099	
GRMZM5G834455	187379121	187379438	
GRMZM2G142507	187380518	187384704	
GRMZM2G441888	187383447	187384622	Photosystem II PsbP, oxygen evolving complex
GRMZM2G142597	187387273	187397432	RNA recognition motif domain
GRMZM2G441903	187398921	187400738	Zinc finger, AN1-type
GRMZM2G142638	187403377	187407974	Poly(A) polymerase, central domain
AC212463.3_FG009	187435427	187436221	
GRMZM2G020478	187441277	187443050	Serine/threonine- / dual specificity protein kinase, catalytic domain
GRMZM2G132763	187587612	187591058	Leucine-rich repeat
GRMZM2G132748	187626539	187627195	NADH:ubiquinone oxidoreductase, ESSS subunit
GRMZM2G132704	187635249	187640520	Dilute
GRMZM2G132623	187641040	187642585	Ribosomal protein L31e
GRMZM2G435224	187641060	187642612	
GRMZM2G132607	187643004	187646940	Carbohydrate kinase PfkB
GRMZM2G563405	187649672	187650116	
GRMZM2G141320	187667515	187670309	Diacylglycerol glucosyltransferase, N-terminal
GRMZM2G040129	187753619	187755711	DNA-directed DNA polymerase, family B, mitochondria/virus
GRMZM2G580853	187842642	187843102	
GRMZM2G163771	187843888	187844570	
GRMZM2G163783	187845063	187845576	
GRMZM2G121302	187877315	187877869	Cyclophilin-like peptidyl-prolyl cis-trans isomerase domain
GRMZM5G873791	187877340	187877853	

GRMZM2G121312	187883668	187885516	Leucine-rich repeat-containing N-terminal, type 2
GRMZM2G121398	187889142	187892150	
GRMZM5G839014	187975033	187977356	Ovarian tumour, otubain
GRMZM5G836190 (*pan1*)	187978007	187980515	Leucine-rich repeat-containing N-terminal, type 2
GRMZM5G854901	188014689	188017810	tRNA/rRNA methyltransferase, SpoU
GRMZM5G879527	188031610	188034600	Myc-type, basic helix-loop-helix (bHLH) domain
GRMZM2G703846	188036995	188037538	
GRMZM5G861100	188059257	188062957	
AC234203.1_FG009	188060402	188062129	rRNA-processing protein EFG1
AC234203.1_FG010	188063594	188066385	
AC234203.1_FG011	188071750	188073648	Ethylene insensitive 3-like protein, DNA-binding domain
AC234203.1_FG004	188083185	188089513	ABC transporter, transmembrane domain
AC234203.1_FG005	188092362	188092850	
GRMZM5G822593	188114875	188119970	Lipoxygenase, LH2
GRMZM2G161004	188169374	188172490	G-patch domain
GRMZM2G160917	188181863	188185970	Transcription factor, SBP-box
GRMZM2G159263	188256572	188256759	
GRMZM2G413230	188333139	188333371	
GRMZM2G115436	188342737	188344114	
GRMZM2G115442	188344346	188355656	Short-chain dehydrogenase/reductase SDR
GRMZM2G115462	188386434	188386882	Ribonuclease T2-like
GRMZM2G022499	188457694	188461344	SANT/Myb domain
GRMZM2G403669	188600179	188600736	
GRMZM2G403667	188601086	188602301	
GRMZM2G403664	188601935	188602807	
GRMZM2G007681	188719663	188811722	RNA polymerase, N-terminal
GRMZM2G325543	188733228	188736419	Zinc finger, BED-type predicted
GRMZM2G430455	188855847	188859402	KOW
GRMZM2G130659	188880026	188886014	Nonaspanin (TM9SF)
GRMZM2G430522	188906106	188908967	No apical meristem (NAM) protein
GRMZM2G467263	188927396	188928192	
GRMZM2G168669	188928450	188929193	
GRMZM2G342437	188983389	188985663	
GRMZM2G042622	188986180	188988366	Serine-threonine/tyrosine-protein kinase catalytic domain
GRMZM5G847243	189045340	189045985	
GRMZM2G357919	189077793	189078897	Protein kinase, catalytic domain
GRMZM2G055992	189081768	189085843	Leucine-rich repeat

GRMZM2G056056	189088108	189090646	
GRMZM2G056122	189091152	189093163	Pentatricopeptide repeat
GRMZM2G088627	189145769	189150346	Peptidase M20
GRMZM2G009009	189188469	189190473	
GRMZM2G009117	189191520	189193031	Heavy metal-associated domain, HMA
AC186691.4_FG009	189196177	189197677	
GRMZM2G009154	189200093	189201905	Glycosyl-phosphatidyl inositol-anchored, plant
GRMZM2G308873	189200780	189201223	
GRMZM2G158182	189276877	189277368	
GRMZM2G458441	189278497	189283529	Peptidase C54
AC186691.4_FG003	189334539	189334808	